Advanced Steel Construction – Vol. 18 No. 3 (2022) 715–727
DOI:10.18057/IJASC.2022.18.3.9

EXPERIMENTAL STUDY OF HYSTERETIC BEHAVIOR OF RESILIENT PREFABRICATED STEEL FRAMES WITH AND WITHOUT INTERMEDIATE COLUMNS

Meng-Yao Cheng [1], Yan-Xia Zhang [1, 2, *], Zhen-Xing Li [1] and Wen Wen [1]

[1] *School of Civil and Transportation Engineering, Beijing University of Civil Engineering and Architecture, Beijing, China*

[2] *Beijing Energy Conservation & Sustainable Urban and Rural Development Provincial and Ministry Co-construction Collaboration Innovation Center, Beijing University of Civil Engineering and Architecture, Beijing, China*

** (Corresponding author: E-mail: zhangyanxia@bucea.edu.cn)*

ABSTRACT

The research innovatively proposed a seismic resilient structural system including a prefabricated self-centering steel frame (PSC) and an intermediate column with a friction damper (CD). The CD, installed in the mid-span beam of the PSC, was expected to provide additional stiffness and damping, The seismic performance of the newly-developed resilient structural system thus can be greatly improved. This paper stated the experimental study on the hysteretic behaviors of the newly-developed system. Comparative pseudo-dynamic tests were conducted for the validation where two systems, a PSC with CD and a PSC without CD, were tested respectively. The testing results indicated that a PSC with CD has better seismic performance for long-span structures under catastrophic earthquakes' attack. The CD overall provided additional stiffness for requirements of earthquake fortification criteria. The friction damper, part of CD greatly improves the damping effect together with the energy-dissipation bolts. The small residual rotations of beam-column connections on the PSC subsystem provides a satisfactory self-centering mechanism. Moreover, the steel strands of the resilient structural system can maintain the elasticity even after the highest-intensity earthquake. In turn, the satisfactory seismic performance of the proposed PSC with CD structural system validated. This research developed a series of design formula for the T-plate and L-plate friction damper in the CD to guarantee the designed seismic performance of the proposed seismic resilient structural system. The theoretical hysteresis curve of the system was proposed for the future design specification.

ARTICLE HISTORY

Received: 14 August 2020
Revised: 10 July 2021
Accepted: 8 June 2022

KEYWORDS

Seismic performance;
Pseudo-dynamic test;
Resilient prefabricated steel frame;
Friction damper;
Comparative analysis

1. Introduction

Self-centering steel resilient frames (SC-SRFs) are trends of future seismic resilient structural systems which are known for the self-centering mechanism and the energy-dissipation property. The SC-SRFs can greatly reduce the structural damages through the embedded damping devices, which in turn guarantee the structural reliability for larger-span structures under greater earthquakes. The self-centering mechanism on the other hand improve the structural resilience, which minimizing the cost of structural rehabilitation.

Worldwide scholars proposed various types of SC-SRFs and explored their seismic performance theoretically and experimentally in recent years. The original SC-SRFs were proposed by Ricles et al. [1] which were composed of steel frames, bolted connections, steel strands and steel angles. The bolted connections of the SC-SRFs demonstrated the similar rigidity as welded connections [2-5]. The strands and anchorages provide proper self-centering mechanism. The steel angles offer energy-dissipation properties to ensure the elastic performance of major structural members, e.g. beams and columns. Numerical simulations were conducted to conclude damage identification criteria. The researchers proposed various methods to improve the damping of the system by replacing the steel angles with energy-dissipation rods [6], frictional devices [7-10], and brass-plate -dissipation devices [11].

The steel frames require satisfactory lateral stiffness for the overall structural system. Thus, an intermediate column with dampers (CD) were designed to install in-between a steel frame. Experimental research [12-14] were conducted to study its mechanical properties and seismic effects. The setting of CD can effectively reduce the displacement response of the frame.

The steel strands require in situ pretension during installation on the self-centering frame which was unsafe and costly. The research group [15-19] proposed an prefabricated self-centering steel frame (PSC) where the steel strands were prestressed before erection. An innovative seismic resilient structural system, a CD connected to PSC were proposed [20] to satisfy the seismic performance and earthquake fortification criteria. The newly-developed system was also economic and safe for structural erections.

2. Design and analysis of PSC-CD resilient structural system

2.1. Design of PSC-CD

The PSC (Fig. 1) comprises three components: the fixed column, the flexible beam, and the self-centering connections with post-tensioned steel strands and friction bolts [18]. The PSC requires additional lateral stiffness for larger-span structures. The CD, therefore, is proposed where an intermediate column with a friction damper is connected to the mid-span of the beam in the PSC (Fig. 2). The friction damper is placed in-between the upper and lower columns where a T-shape steel plate connecting to the upper column, and two L-shape steel plates connecting to the lower column (Fig. 3(a)). The T-shape plate has two rows of elongated holes, and the L-shape plates has 2 by 2 holes aligned with the elongated holes. Two brass plates are squeezed by the T-shape and L-shape plates. The frictional high-strength bolts are installed to connect the plates and dissipate energy through sliding along the elongated slotted holes (Fig. 3(b)).

The friction damper functions when the external load exceeds the maximum static frictions and the connections transmit the internal force steadily. The fluent transmission of the connections requires the stiffness of the CD satisfying following criteria: 1) the CD provides additional stiffness to the PSC; 2) the connections sustain external loads together with the PSC; 3) the friction damper provides effective stiffness in comparison with overall stiffness of the PSC. Overall, the CD maintain elastic states and the loads are transmitted to the friction damper.

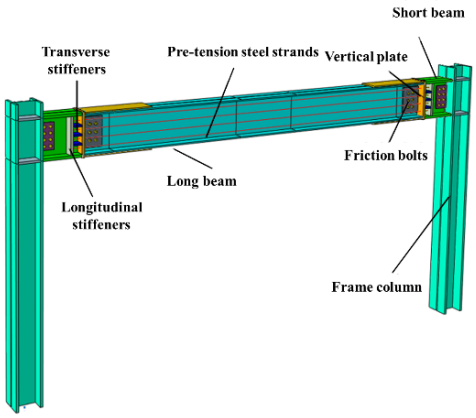

Fig. 1 Details of PSC

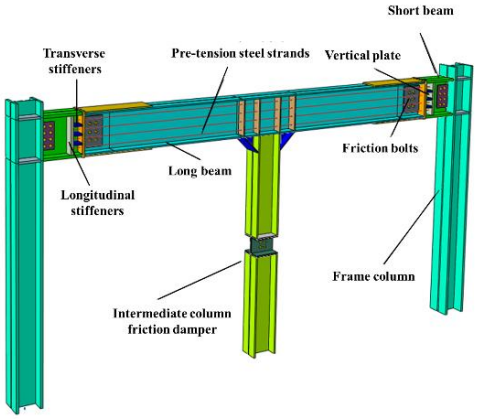

Fig. 2 Details of PSC-CD

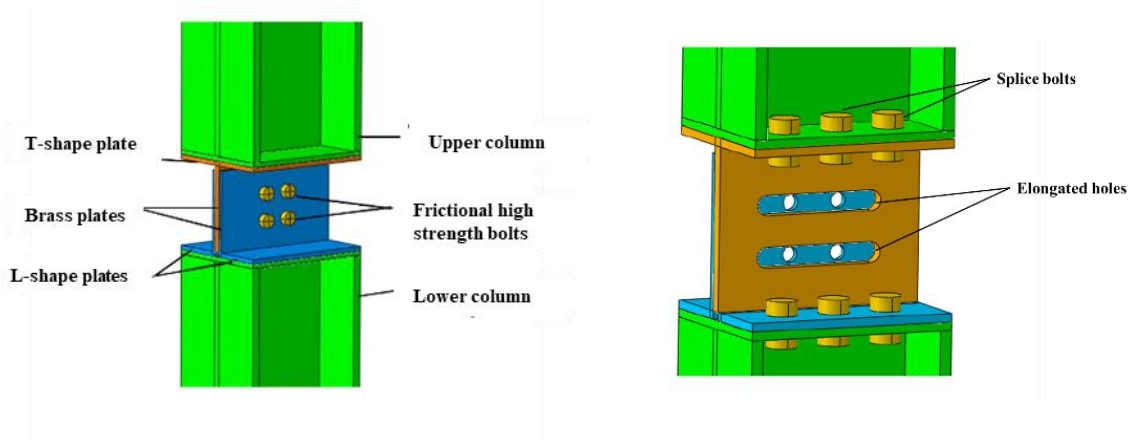

(a) details of CD (b) details of friction dampers

Fig. 3 Design of CD

2.2. Theoretical analysis of PSC-CD

Gaps exist in-between the T-shape plate and the lower connecting component, and the L-shape plates and the upper connecting components as shown in Fig. 4. The upper column and the lower column are designed to be straight and vertically. The friction damper has no initial deviation in rorations and translations. Under the assumptions, the minimum distance of the gaps are calculated as following:

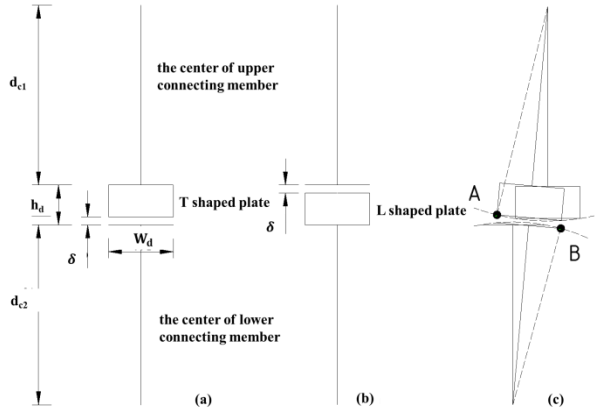

Fig. 4 Structural details of friction dampers

$$\delta \geq d_{c1} + h_d - \sqrt{(2d_{c1} + h_d - \sqrt{(\frac{W_d}{2})^2 + d_{c1}^2})^2 - (\frac{W_d}{2})^2} \quad (1)$$

$$\delta \leq h_d \quad (2)$$

$$d_{c1} = d_{c2} \quad (3)$$

where
d_{c1} is the height of the upper column;
d_{c2} is the height of the lower column;
W_d is the width of the CD;
h_d is the height of the friction damper;
δ is the distance of the gaps.

The T-shape plate and L-shape plates are required to maintain elasticity and sustain the friction without deformation. The T- and L-shape plates should meet the following criteria:

$$\frac{3F_{max}}{2t_T \times W_d} < f_V \quad (3)$$

$$\frac{3F_{max}}{4t_L \times W_d} < f_V \quad (4)$$

where
t_T is the thickness of T-plate;
t_L is the thickness of L-plate;
f_V is the shear strength of the steel;
F_{max} is the friction;
W_d is the modulus of section.

2.3. Theoretical hysteresis curve of PSC-CD

The performance of PSC-CD under cyclic loads are carefully analyzed theoretically. The CD provides additional stiffness through frictions with small

shift. As the lateral displacement of PSC-CD increases, the frictions of the friction damper increases till the maximum value achieved. The CD can still provides additional stiffness as the self-centering connections start to work, i.e. the gap between the fixed connection and flexible beam appears. Based on this qualitative analysis, the hysteresis curve of the PSC-CD is proposed with the zigzag shape as shown in Fig. 5.

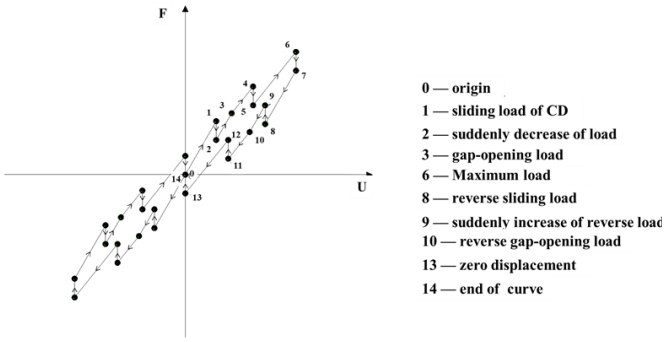

Fig. 5 Theoretical force displacement curve of PSC-CD

The origin indicates that the frame is located in its original state. Point 1 indicates that the load transmitted to the CD reaches the maximum friction and the friction damper starts to slide. The upper and lower columns of the CD suddenly changed from a vertical state to an inclined state. The additional stiffness provided by the CD thus disappeared observed from point 1 to 2 where a drop occurred. The stiffness at segment 2-3 resembles to that at segment 0-1. Point 3 indicates that the self-centering connection starts to work where the stiffness of the frame decreases. The stiffness at segment 3-4 is mainly provided by the frame. Point 6 indicates the loading capacity of the PSC-CD, and a drop appears from segment 6 to segment 7 represents the maximum friction achieved and the CD slides. Point 8 represents that the loads taken by CD reach the sliding friction in reverse and the additional stiffness suddenly disappears. The external load suddenly increases and the increase value is equal to the sliding load. The stiffness of segment 7 to 8 is consistent with that of segment 0 to 1. Point 10 indicates that the gap openings of the connections begin to close, the segment 10-11 show the stiffness of the entire structure decreases similar to that at segment 3-4. Point 13 indicates that the gap of connection is completely closed, and the damper reaches the sliding load. The curve suddenly returns to points 14, the origin.

3. Experimental design

3.1. Experimental prototype

A 3x5 four-story prefabricated resilient steel structure (Fig. 6) is designed with requirement of 50-year service life and 2nd-rank safety level according to the structural properties of the resilient frame and the specification of seimic design [21]. The prefabricated resilient steel structure is located in Beijing, China. The seismic fortification intensity is at level 8, the designed acceleration is 0.2 g, and the site category is level III. The dead load of the floor is 7.0 kN/m^2 and the live loads of floors and roofs are both 2.0 kN/m^2. The snow load is 0.45 kN/m^2. The first-story height is 3.9 m and that of other floors is 3.6m. General beam-column connections are hinged. The frames circled by magenta boxes are the designed resilient prefabricated steel frames. The dimension of the frame column and beam are □400×400×34 mm and H588×300×12×20 mm, respectively. The cross sections of upper and lower columns of the CD are H400×500×20×24 mm. Four M20 high-strength frictional bolts are used in the friction damper. The post-tensioned (PT) high-strength steel strands is 1×19 with the nominal diameter, 21.6mm and the nominal area, 285mm^2. The ultimate strength of the strands is 1860 Mpa.

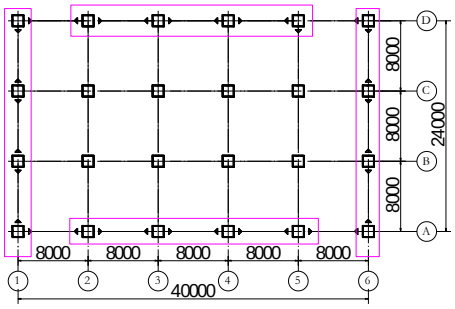

Fig. 6 The plane diagram of prototype structure

A resilient prefabricated steel frame is selected as a prototype. The study is composed of two parts, i.e. experimental testing and numerical simulations. The first floor is selected for experimental study. The upper floors are studied numerically (Fig. 7). This paper only focus on the experimental study.

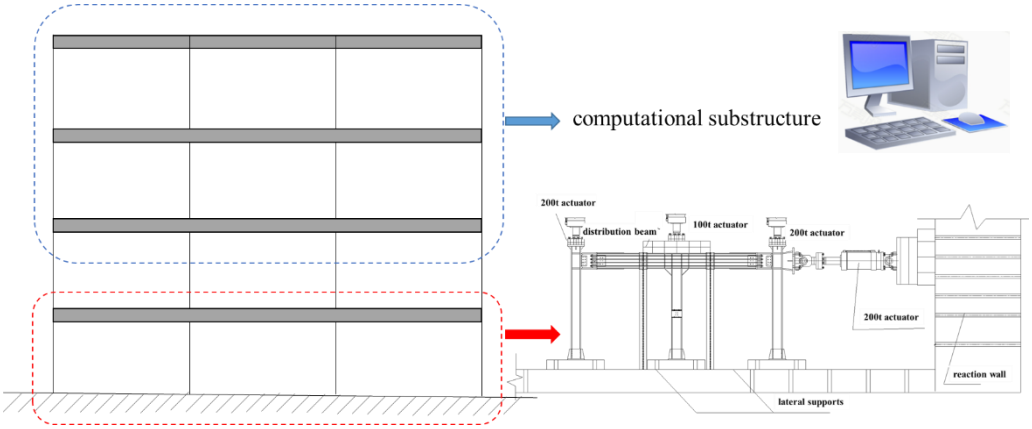

Fig. 7 Substructures of pseudo-dynamic test

3.2. Experimental structures

The model structure is scaled 0.75 times to the dimension of the prototype and the axial compression ratio is same to the prototype [22]. The detailed dimensions of PSC and PSC-CD are shown in Fig. 8. The story height is 3.15 m and the span is 6 m. The sizes of two testing specimens are as follows: the dimension of column is H300×300×20×30 mm and the thicknesses of column stiffening ribs are 30 mm. The length of long beam(H450×250×14×16 mm) and short beam (H482×250×14×30 mm) are 4740 mm and 450 mm, respectively. The thicknesses of the transverse and the longitudinal stiffening ribs are 30 mm and 20 mm. The cover plates, 800×220×16 mm, are set up on the two ends of the long-beam flanges. The dimension of the vertical plate is 500×250×30 mm, and the frictional plates are welded on the outer surface of the column flange whose dimension is 300×175×14 mm. The thickness of brass plate is 3 mm. Six energy dissipating bolts which connect the short-beam and long-beam adopt M24 high-strength bolts [23] and the eight high-strength bolts which connect the column and short-beam are M20 bolts. Eight 1 × 19 steel strands are selected in each frame beam with the value of the initial PT force for single steel strand of 0.25T_u. The size of the connection components for intermediate column is H300×250×16×18 mm and the 4 friction-type high strength bolts of the frictional damper are M16 bolts.

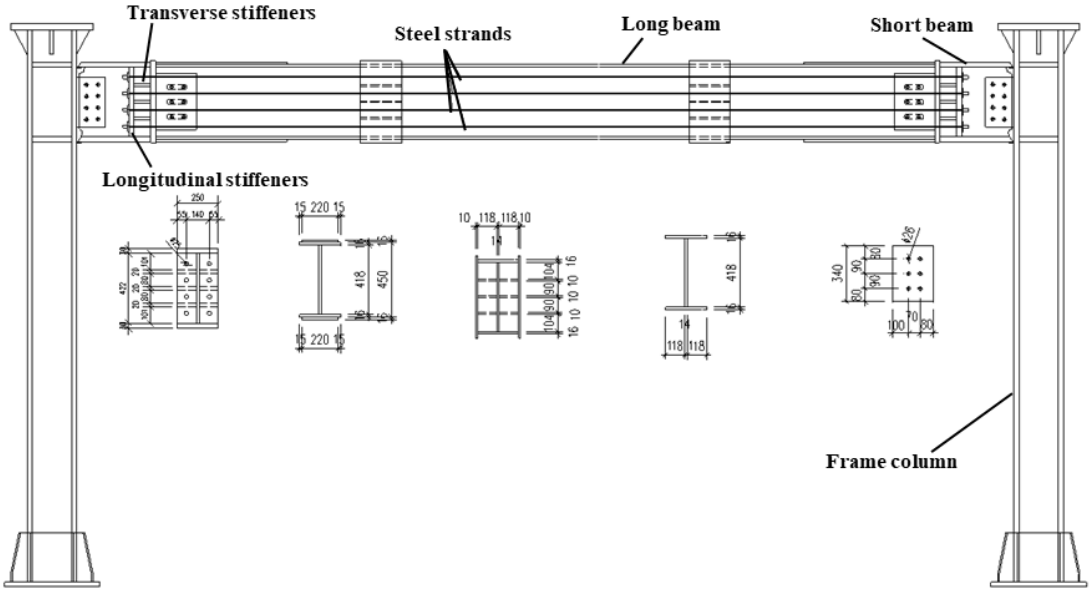

(a) Detailed diagram of PSC

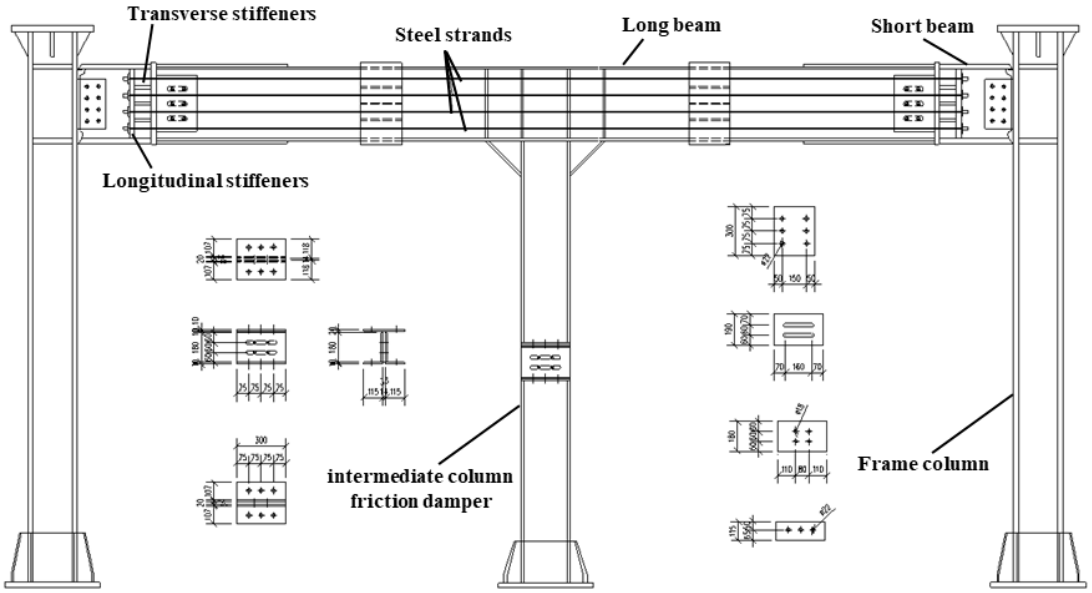

(b) Detailed diagram of PSC-CD

Fig. 8 Detailed diagram of specimens

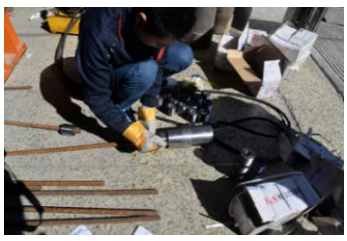

(a) Fix the wedges in the end of strands

(b) Install the sensors in the end of strands

(c) Preloaded in the stressing end

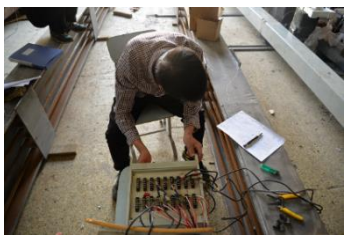

(d) Monitor the variation of cable force

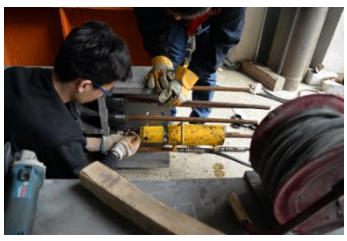

(e) Adjust the cable force

(f) Cut the redundant lengthof steel strands

Fig. 9 The whole process of tensioning steel strands

(a) Installation of beam and column of the model structure

(b) Installation of CD of the PSC-CD model structure

Fig. 10 Installation procedures of PSC-CD

The short and long beams of the resilient prefabricated steel frame are connected by 8 PT high strength steel strands. The steel strands are post-tensioned on ground level instead of that in the air. This technique is safe and economic which is conducted as follows (Fig. 9): 1) the long beam and short beam are connected through the frictional plates and bolts; 2) steel strands are fixed through the holes with pressure sensors are mounted on the anchors at both ends; 3) steel strands are initially tensioned to the 70% of the designed values at one end with the other end fixed; 4) the steel strands achieved its targeted force in the second tensioning. The whole post-tension technique thus achieved.

The model structure is built up. The columns are bolted to the ground through the hold-down. A shear plate is welded to the hanging end of the column. The beam, i.e. long beam connected with the short beam, is installed to the columns through bolting and welding. The web of the beam is tightly connected to the shear plate on the column. Two flanges of the I-section beam are angle welded to the column. Thus the PSC model structure is set up (Fig. 10(a)).

Regarding to the PSC-CD model structure, the upper column is mounted on the long beam firstly. The lower column of the CD is installed through hold-down similar to other columns. The friction damper bridges the lower column to the upper column via the T-shape an L-shape plates' combinations. The high-strength frictional bolts are eventually tightened and the entire PSC-CD model structure is completed (Fig. 10(b)).

3.3. Material properties

The model structures, i.e. PSC and PSC-CD are made of Q345B steel [24]. Three types of material testing are conducted: steel-tensile tests, steel-strands tests and plate-friction tests.

The tensile tests prepare 6 types of coupons categorized by the thickness. Each types of coupons have 3 testing samples. The coupon tests are tested by the universal material testing machine. The material properties of Q345B steel used in the experiment are shown in the Table. 1.

Three steel strands are stretched in the steel-strands tests. The steel strands are cut from the long steel strands and place in the universal material testing machine for testing. The material properties of steel strands are shown in Table. 2.

The brass plates in the frictional damper is designed to dissipate energy through frictions between brass and steel. The plate-friction tests are set up for the frictional damper embedded in the CD. The specimen is made of two brass plates and a steel plate in-between (Fig. 11(a)). The frictional coefficient between the steel- and the brass- plates range from 0.34 to 0.38. The hysteresis curve of the test is shown in Fig. 11(b).

Table 1
Material test of Q345B

Material	Thickness (mm)	E ($\times10^5$N/mm^2)	Yield strength (N/mm^2)	Ultimate strength (N/mm^2)	Elongation percentage (%)
Q345B	12	2.08	435	570	27
	14	2.05	384	561	24.15
	16	2.1	392	555	24.05
	18	2.09	381	555	24.5
	20	2.1	384	550	26.95
	30	2.07	350	505	28.05

Table 2
Material test of steel strands

Steel strands	Specimen	E($\times10^5$N/mm^2)	Yield strength/(N/mm^2)	Tensile strength (N/mm^2)
1×19	Specimen1	2.03	1728.3	1894.5
	Specimen2	2.05	1727.1	1895.8
	Specimen3	2.00	1732.8	1875.4
	Average	2.03	1729	1889

(a) Friction test of brass plates

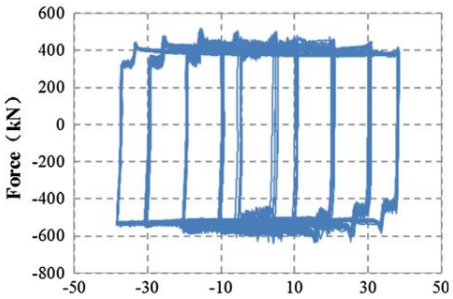

(b) Force-displacement hysteresis loops

Fig. 11 The friction experiment of Q345B steel and brass plates

3.4. Testing set-up

The 200-ton horizontal actuator mounted on the reaction wall provides lateral loads to the specimen under the displacement command by the computer. Two 200-ton hydraulic jacks are placed on the top of two columns, providing 756 kN axial compression. A distribution beam is place in the mid-span of

beams of the model structures. The 100-ton hydraulic jack simulates the live load together with a distribution beam and loads at the frame beam with 96 kN. Two lateral supports at the 1/3- and 2/3-span prevent the out-of-plane buckling of the frame beam (Fig. 12).

The pseudo-dynamic testing are conducted for both PSC and PSC-CD through the multi-story structural remote-control hybrid pseudo-dynamic testing platform (NestSLab_MSBSM1.0.0). The commanded displacement is integrated from accelerations of a selected seismic signal considering both the experimental substructure and the numerical substructure. Floor weights and theoretical hysteretic curves are input for the numerical substructures. The damping ratios of each floor are set as 0.05 for the testing in the platform. The stiffness before and after the opening of self-centering beam-column connections, i.e. K_1 and K_2, are obtained from the numerical simulations of the model structures, same to those displacement d_1 and d_2 of the entire model structures (Table. 3&4). The selected seismic waves are El-Centro and Wenchuan (Fig. 13 and Fig. 14). The peak accelerations of selected waves are scaled as 0.07g, 0.2g, 0.4g, 0.51g, 0.62g, 0.8g, 1.0g corresponding to different earthquake intensities: frequent-, fortification-, rare-, medium-rare, 9-degree rare-, and extreme-rare intensities according to the specification [21]. The time steps of the original waves are 0.01s and those of the input waves are scale to 0.0086s for the 0.75-time model structures. The response spectrum of the waves are shown in Fig. 15.

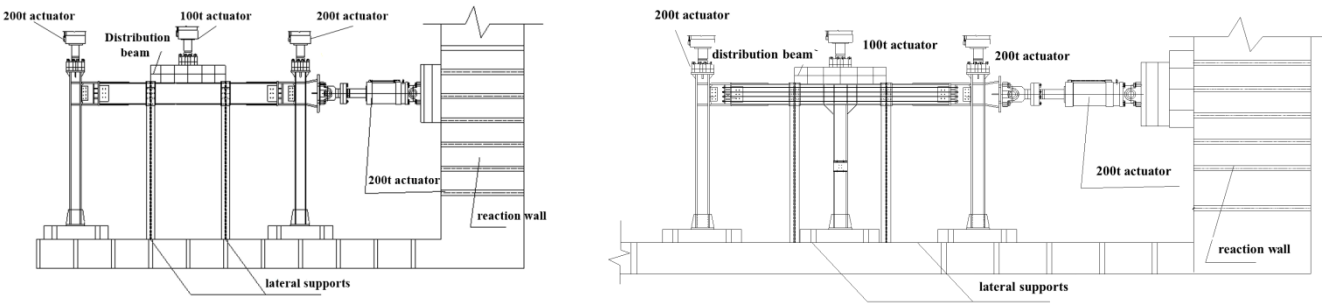

(a) PSC (b) PSC-CD

Fig. 12 Diagrammatic sketch of loading

Table 3
Input parameters of the test

Story	M (t)	K_1 (kN/m)	K_2 (kN/m)	d_1 (mm)	d_2 (mm)
4	162	14176	3677	24.0	20.0
3	162	14178	3676	24.9	20.3
2	162	13376	3692	21.6	20.3
1	162	28449	10988	29.0	23.6

Table 4
Input parameters of pseudo-dynamic test for resilient prefabricated steel frame with intermediate column friction damper

Story	M (t)	K_1 (kN/m)	K_2 (kN/m)	d_1 (mm)	d_2 (mm)
4	170	31600	4990	16.2	29.2
3	170	34327	6087	16.2	29.2
2	170	32295	8839	16.2	29.2
1	170	38313	10512	12.5	25.0

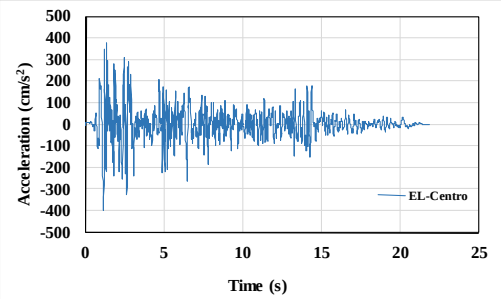

Fig. 13 Time history curve of EL-Centro

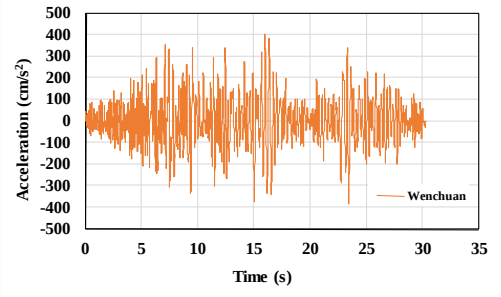

Fig. 14 Time history curve of Wenchuan

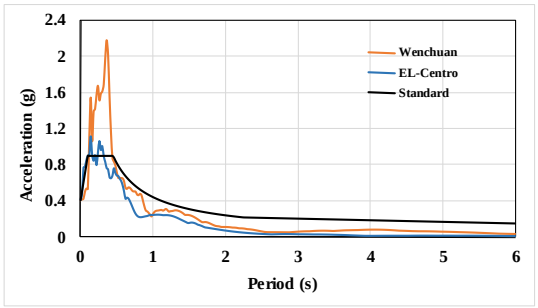

Fig. 15 Response spectrum

3.5. Measurement set-up

3.5.1. Cable force and bolt load

Pressure sensors (Fig. 16 (a)) are placed at one ends of the steel strands to record variations of cable forces ranging up to 500 kN during the loading process. The bolted forces of CD are measured by pressor sensors ranging up to 300 kN (Fig. 16 (c)).

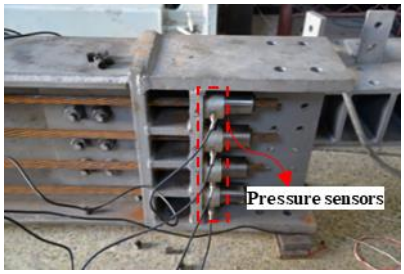

(a) Force sensor

(b) Pressure sensor

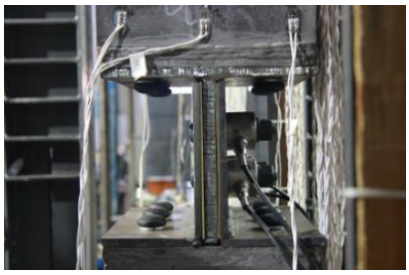

(c) Bolt sensor

Fig. 16 The setup and appearance of sensors

3.5.2. Displacement

The measurement of displacement mainly includes the following aspects, and the layout diagrams are presented in Fig. 17.

(1) Displacements of frames: the displacement sensors of the horizontal actuator measures the lateral displacements of the model structures. The displacement meters ranging up to 150 cm are placed at the left/right upper flanges of the columns. The displacements of the top of the column are measured. The other displacement meters are placed at the base of the columns and measure the slippages.

(2) Gap-openings: the gap-opening of connections are monitored by the resistance displacement meters whose range is up to 40 mm. The meters were installed at the inner sides of upper and lower flanges of the long beam.

(3) Displacements of the CD: the displacement meters ranging up to 50 cm are allocated at the base of the CD. The horizontal slippages at the bottom of the lower column are measured. Two displacement meters are placed at the upper and lower columns of CD, adjacent to the friction damper. The ranges of these meters are up to 150 cm. The distance of gap opening of the friction damper thus is calculated as the difference between displacements of the upper and lower columns.

3.5.3. Strain

Strain gauges are installed on the various positions of the specimens (Fig. 18): flanges and bases of columns, flanges of the beam, upper and lower columns of the CD (Fig.18 (b)). Three-way strain gauges are used to measure the web of frame columns and that of the CD.

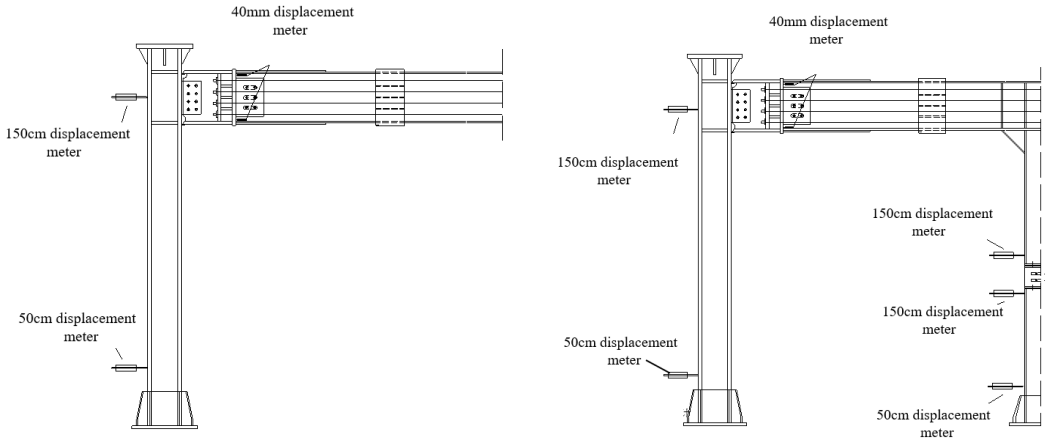

(a) Layout of displacement meter for PSC

(b) Layout of displacement meter for PSC-CD

Fig. 17 Layout diagrams of displacement meter

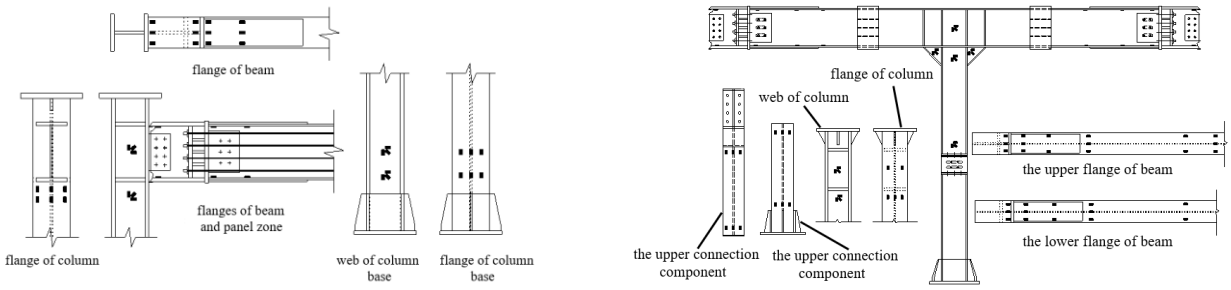

(a) Arrangement of strain gauges for PSC

(b) Arrangement of strain gauges for PSC-CD

Fig. 18 The detailed arrangement of strain gauges

Table 5
The variation of maximum displacement response

	Items	0.07g	0.20g	0.40g	0.51g	0.62g	0.80g
PSC	+ (mm)	5.22	15.50	34.50	46.30	46.70	66.70
	Interstory drift (1/rad)	563	190	85	63	63	44
	- (mm)	7.81	23.02	35.12	45.10	58.05	65.02
	Interstory drift (1/rad)	376	129	84	65	51	45
PSC-CD	+ (mm)	7.00	19.60	29.30	32.40	45.40	61.80
	Interstory drift (1/rad)	420	150	100	91	65	48
	- (mm)	8.20	16.80	26.90	31.50	30.80	39.80
	Interstory drift (1/rad)	359	175	109	93	95	74

4. Experimental study

4.1. Displacement response

The time history curves of the variation of displacement response for PSC and PSC-CD under the action of Wenchuan wave is shown in Fig. 19. The displacement response under Wenchuan wave is greater than that under EL-Centro wave. The analysis presented in this paper mainly focus on the Wenchuan wave. The maximum horizontal displacements are listed in Table. 5.

The inter-story drifts of both PSC and PSC-CD were less than the elastic limits, i.e. 1/250 required by the specification [25], under the attack of 8-degree frequent earthquake. However, the drifts of both systems were beyond the elastic inter-story limits but within the plastic inter-story drift (1/50) when the amplitudes of Wenchuan wave were as strong as 8-degree fortification and rare earthquakes.

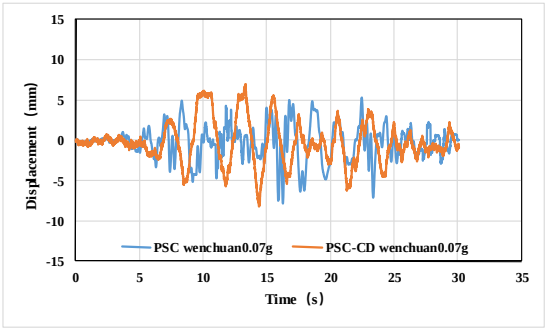

(a) In the condition of frequent earthquake(0.07g)

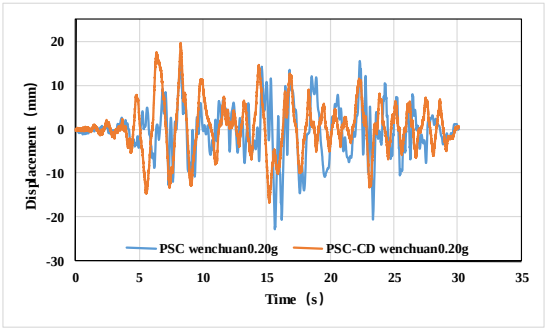

(b) In the condition of fortification earthquake (0.02g)

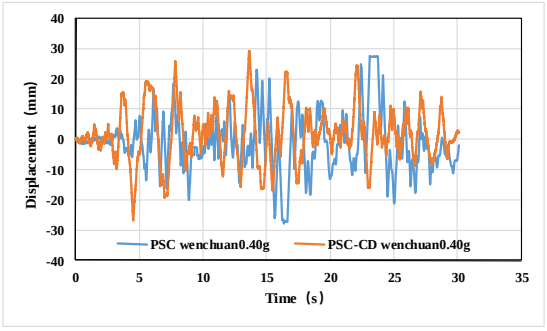

(c) In the condition of rare earthquake (0.40g)

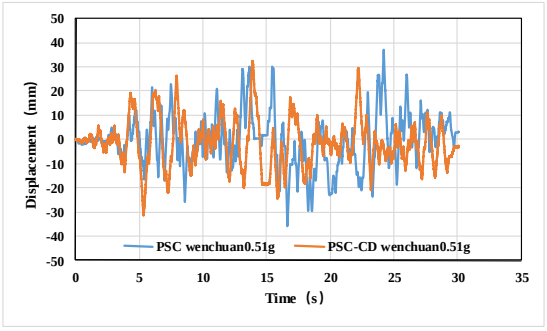

(d) In the condition of 8-degree rare earthquake (0.51g)

Fig. 19 Displacement time history curves for PSC and PSC-CD under the action of Wenchuan wave

(a) Column interstory at 1/84 for PSC

(b) Column interstory at 1/100 for PSC-CD

Fig. 20 Photographs of lateral displacement for columns under the actions of Wenchuan (PGA=0.04g)

(a) Column interstory at 1/63 for PSC

(b) Column interstory at 1/91 for PSC-CD

Fig. 21 Photographs of lateral displacement for columns under the actions of Wenchuan (PGA=0.51g)

4.2. Gap-opening

The gap openings of beam-column connections demonstrate the structural performances of the systems. The values of gap-opening for PSC and PSC-CD are listed in Table. 6. The beam-column connections remained stills during the 8-degree frequent earthquake. Small gaps showed when the amplitudes of the Wenchuan wave reached 8-degree fortification earthquake.

The gap openings developed as the amplitudes of Wenchuan wave increased from 0.2g to 1.0g (Table. 6). The maximum rotations are 0.514% for PSC and 0.344% for PSC-CD when the acceleration is 0.51g. The rotations reach 1.547% for PSC and 0.933% for PSC-CD as the acceleration is 1.0g. The PSC-CD show its advantages as the earthquake go stronger.

On the other hand, the residual gap-opening rotations of the PSC-CD remain smaller compared to that of the PSC. The residual gap-openings are 0.033% for the PSC but 0% for the PSC-CD at acceleration 0.51g. The PSC has 0.029% residual gap-opening when the acceleration is 1.0g. The PSC-CD is only 0.011%. The CD provides the additional lateral stiffness and damping to protect the beam-column connections thus strengthen the overall steel frames eventually.

Table 6
The maximum and residual gap-opening

Items	PGA		Maximum gap-opening		Residual gap-opening		Maximum gap-opening rotation		Residual gap-opening rotation	
			-	+	-	+	-	+	-	+
			mm	mm	mm	mm	rad%	rad%	rad%	rad%
PSC	0.20g	EL-Centro	0.31	0.23	0.040	0.008	0.068	0.052	0.009	0.002
		Wenchuan	0.41	0.35	0.013	0.025	0.090	0.078	0.003	0.006
	0.40g	Wenchuan	1.30	0.82	0.130	0.135	0.289	0.181	0.029	0.030
	0.51g	Wenchuan	2.32	0.86	0.150	0.090	0.514	0.192	0.033	0.020
	0.62g	Wenchuan	4.63	1.21	0.030	0.013	1.028	0.268	0.007	0.003
	0.80g	Wenchuan	5.60	2.03	0.020	0.023	1.243	0.451	0.004	0.005
	1.0g	Wenchuan	6.96	2.87	0.075	0.133	1.547	0.637	0.017	0.029
PSC-CD	0.20g	EL-Centro	0.5	0.15	0	0	0.111	0.033	0	0
		Wenchuan	0.6	0.3	0	0	0.133	0.067	0	0
	0.40g	Wenchuan	1.3	0.5	0	0.05	0.289	0.111	0	0.011
	0.51g	Wenchuan	1.55	0.7	0	0	0.344	0.156	0	0
	0.62g	Wenchuan	1.9	1.1	0	0	0.422	0.244	0	0
	0.80g	Wenchuan	2.8	1.95	0.05	0.1	0.622	0.433	0.011	0.022
	1.0g	Wenchuan	4.2	2.15	0	0.05	0.933	0.478	0	0.011

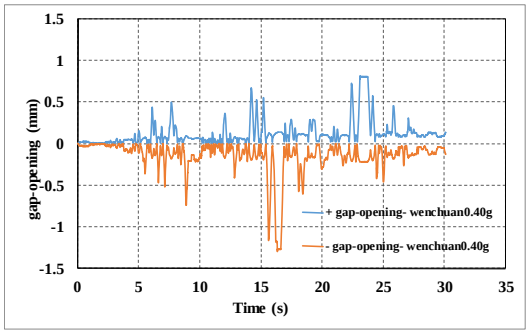

(a) Gap-opening of PSC (Wenchuan 0.40g)

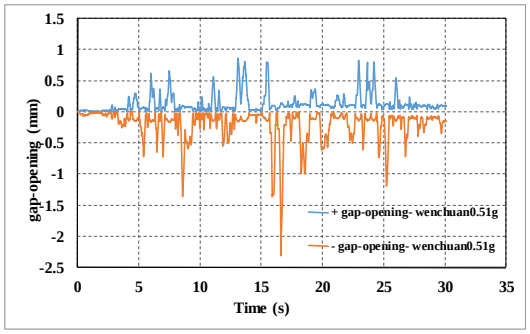

(b) Gap-opening of PSC (Wenchuan 0.51g)

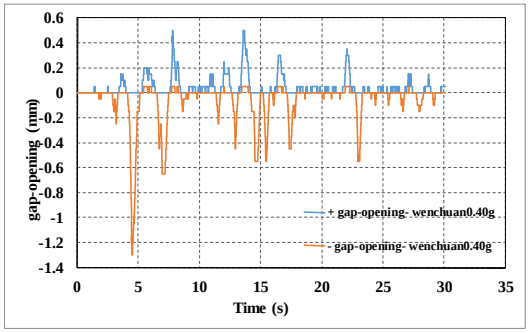

(c) Gap-opening of PSC-CD (Wenchuan 0.40g)

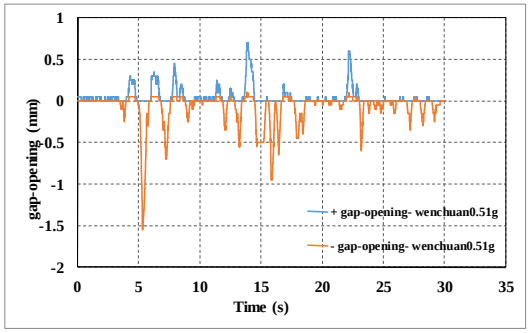

(d) Gap-opening of PSC-CD (Wenchuan 0.51g)

Fig. 22 Time history curves of gap-opening for PSC and PSC-CD

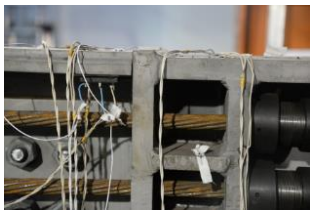

(a) Gap-opening of PSC (0.40g)

(a) Gap-opening of PSC (0.51g)

(c) Gap-opening of PSC-CD (0.40g)

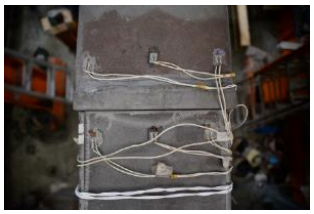

(d) Gap-opening of PSC-CD (0.51g)

Fig. 23 The photographs of gap-opening for PSC and PSC-CD under Wenchuan waves

4.3. Cable force

Table. 7 presents the variations of cable force in different seismic accelerations. It lists the initial values, maximum values, minimum values during the testing and the final values at the end. The ultimate tensile strength of steel strands T_u is 591kN presented in the previous section. In the condition of 8-degree frequent earthquake, the cable force is unchanged as no openings at the connections. In the condition of 8-degree fortification earthquake, cable force increases slightly. In the condition of rare earthquake, the maximum cable forces for PSC and PSC-CD are $0.266T_u$ and $0.277T_u$ respectively. The cable forces recover to the initial values after loading in each case of the seismic accelerations as shown in Table. 7. Under the action of seismic waves whose peak acceleration is in the range of 0.62g to 1.0g, the increases of cable forces for PSC are greater than that of PSC-CD as the greater gap-openings are generated. The variations of cable force have the same tendency with gap openings. The systems are resilient after earthquake as PT steel strands are used. After the test, the maximum accumulative decreases for PSC and PSC-CD were 9.79% and 4.98%. The remained PT cable forces demonstrates that the systems, especially the PSC-CD can function and withstand aftershocks in the reality.

Table 7
Variation of cable force

Items	Moment	0.07g	0.20g	0.40g	0.51g	0.62g	0.80g	1.0g
		T_{ave}/T_u	T_{ave}/T_u	T_{ave}/T_u	T_{ave}/T_u	T_{ave}/T_u	T_{ave}/T_u	T_{ave}/T_u
PSC	Initial	0.249	0.248	0.246	0.244	0.238	0.233	0.229
	Maximum	0.250	0.257	0.266	0.275	0.309	0.318	0.335
	Minimum	0.246	0.244	0.241	0.237	0.231	0.227	0.221
	End	0.249	0.248	0.244	0.243	0.236	0.231	0.225
PSC-CD	Initial	0.247	0.256	0.252	0.251	0.250	0.247	0.245
	Maximum	0.261	0.267	0.277	0.282	0.282	0.293	0.316
	Minimum	0.244	0.242	0.241	0.241	0.235	0.235	0.227
	End	0.255	0.250	0.251	0.251	0.247	0.245	0.236

Table 8
Cumulative decreases of cable force

PGA	PSC				PSC-CD			
	EL-Centro		Wenchuan		EL-Centro		Wenchuan	
	Percentage	Force/kN	Percentage	Force/kN	Percentage	Force/kN	Percentage	Force/kN
0.07g	0.11%	0.16	0.13%	0.19	0.58%	0.83	-2.70%	-3.9
0.20g	0.44%	0.63	0.39%	0.56	-3.16%	-4.57	-0.62%	-0.9
0.40g	1.31%	1.9	1.91%	2.77	-	-	-1.01%	-1.47
0.51g	2.01%	2.92	2.55%	3.69	-	-	-1.01%	-1.47
0.62g	4.52%	6.55	5.32%	7.71	-	-	0.69%	1
0.80g	6.35%	9.2	7.10%	10.29	-	-	1.57%	2.27
1.0g	8.24%	11.94	9.79%	14.19	-	-	4.98%	7.2

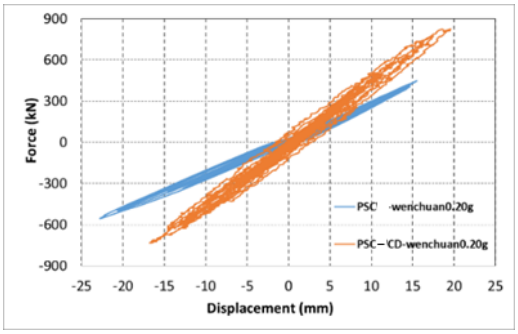

(a) Hysteresis loops of PSC and PSC-CD (0.20g)

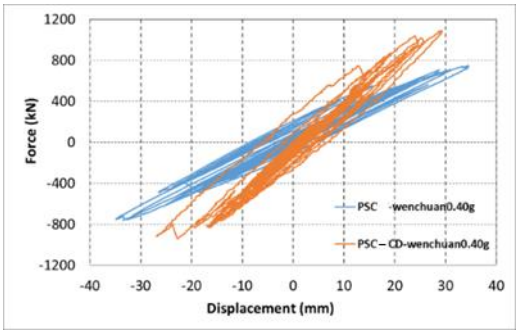

(b) Hysteresis loops of PSC and PSC-CD (0.40g)

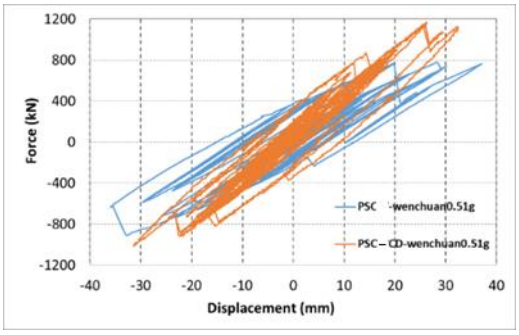

(c) Hysteresis loops of PSC and PSC-CD (0.51g)

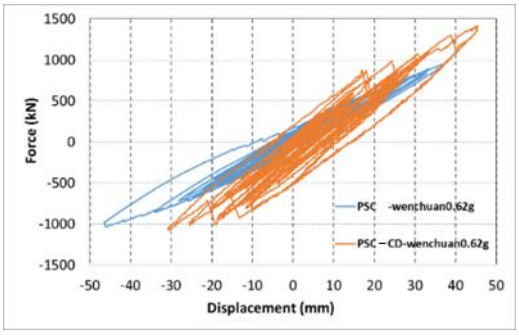

(d) Hysteresis loops of PSC and PSC-CD (0.62g)

Fig. 24 Force-displacement curves of PSC and PSC-CD under the actions of different earthquake (Wenchuan wave)

4.4. Hysteretic behavior

The force-displacement curves of the two frames show the linearity in the elastic states before the 8-degree fortification earthquake. The initial PSC-CD system shows higher initial lateral stiffness compared to the PSC system, 48.20 kN/mm and 30.95 kN/mm respectively.

The hysteresis behaviors of the systems start as the PGA reaches 0.2g (the fortification earthqauake) (Fig. 24 (a)). The inside areas of the hysteresis loops further increase as the PGA increases (Fig. 24). The areas inside the curves of PSC-CD are greater than that of PSC. The energy dissipation capacity of PSC-CD is better than that of PSC. The loading capacity of PSC-CD is much higher than that of PSC in the same condition. Hysteresis loops of PSC-CD appear 'zigzag' shapes due to the discontinuous slippage of friction damper. The existence of CD provides the additional damping. Thus the energy consumption capacity of the PSC-CD improves the steel frame are protected in turn.

4.5. Strain analysis

The maximum values of the strain for some typical locations under the different ground motions are shown in Table. 9. In the condition of 8-degree frequent earthquake and fortification earthquake, PSC and PSC-CD are both in the elastic state. The maximum strains exist in panel zones for frames and flanges for the CD. The main structure is safe.

In the condition of 8-degree rare earthquake, the values of strain increase continuously. Both panel zones of PSC and PSC-CD reach to the plastic stage. The value of PSC is larger than that of PSC-CD over $2\varepsilon_y$ ($\epsilon_y = 2000\mu\epsilon$). The maximum strains locate at the flange of column bases as well as at the beam of the PSC reaching to the plastic stages.

Though the PSC is resilient, the PSC-CD shows better seismic performance with greater lateral stiffness and energy-dissipation capacities. The panel zones of both systems need to be improved and carefully checked. The stiffening ribs can be installed and the thickness of the panel zones can increase.

Table 9
Maximum values of the strain at some typical locations

PGA	Text component	Seismic wave	Flange of column base	Web of column base	Panel zone	Flange of long beam	Flange of short beam	Flange of intermediate column	web of intermediate column
0.07g	PSC	Wenchuan	430	88	909	326	200	0	0
	PSC-CD	Wenchuan	373	180	377	110	65	497	338
0. 20g	PSC	Wenchuan	1006	164	1875	927	851	0	0
	PSC-CD	Wenchuan	393	356	495	199	206	1171	724
0.40g	PSC	Wenchuan	1279	129	4898	1219	1132	0	0
	PSC-CD	Wenchuan	1003	901	3428	714	667	1599	964

Table 10
Slippage of intermediate column

Seismic action	Slippage	
	+/mm	-/mm
EL-C0.07g	1.213	-0.817
Wenchuan0.07g	1.357	-0.522
EL-C0.20g	0.774	-1.316
Wenchuan 0.20g	4.382	-1.484
Wenchuan 0.40g	8.991	-12.157
Wenchuan 0.51g	8.6	-10.5
Wenchuan 0.62g	24.58	-12.64
Wenchuan 0.80g	41.36	-8.54
Wenchuan 1.0g	34.21	-33.65

4.6. Analysis of intermediate column friction damper

4.6.1. Slippage analysis of friction damper

The slippage variations under the action of ground motion are shown in Table. 10 and Fig. 25. The test pictures of slippage of intermediate column under different ground motions are shown in Fig. 27. It can be found that the slippage is too small before 8-degree fortification earthquake. The friction damper of CD provides additional stiffness at this stage and small amount of damping function. The maximum slippage is 4.328 mm. The slippage increases to 12.157 mm under the rare earthquakes (PGA = 0.40g). The friction damper reached to 24.58 mm slippage at large under the PGA = 0.62g seismic wave. The slippage of friction damper increases with the enhance of earthquake effect. The time history of slippage of CD displays in Fig. 26. It can be concluded that the CD originally provides additional lateral stiffness when the intensity of earthquake is small. The friction damper starts working as the seismic energy increase and the displacements of CD arise.

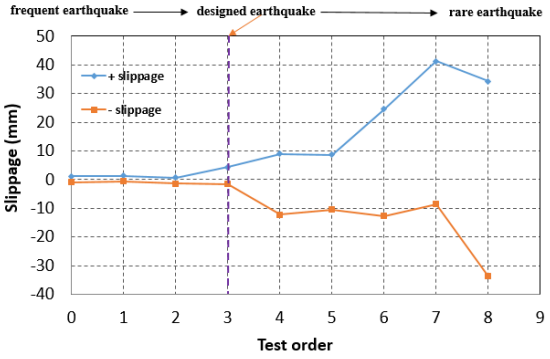

Fig. 25 Slippage under the action of different conditions of ground motion

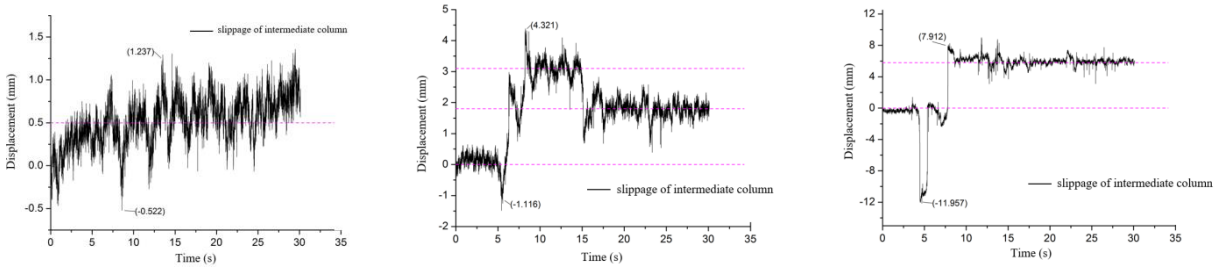

(a) Slippage of CD (0.07g) (b) Slippage of CD (0.20g) (f) Slippage of CD(0.40g)

Fig. 26 Slippage time histories of intermediate column damper

(a) 0.07g

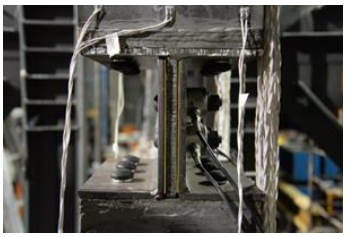

(a) 0.20g

(a) 0.40g

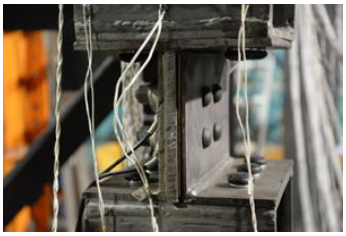

(a) 0.51g

(a) 0.62g

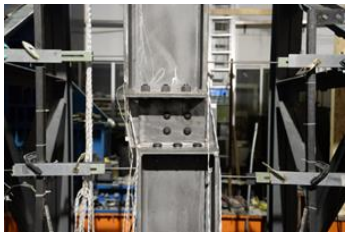

(a) 0.80g

Fig. 27 Slippage of intermediate column under different ground motions

Table 11
Bolt force variations

Seismic action	Moment	0.07g	0.20g	0.40g	0.51g	0.62g	0.80g	1.0g
		P_{los}/P_{ave}	P_{los}/P_{ave}	P_{los}/P_{ave}	P_{los}/P_{ave}	P_{los}/P_{ave}	P_{los}/P_{ave}	P_{los}/P_{ave}
EL-Centro	Initial	0.00%	5.03%	-	-	-	-	-
	Maximum	3.01%	8.63%	-	-	-	-	-
	Minimum	-0.43%	3.35%	-	-	-	-	-
	End	2.40%	6.49%	-	-	-	-	-
Wenchaun	Initial	2.40%	6.49%	14.97%	12.98%	17.32%	21.20%	27.89%
	Maximum	4.27%	14.56%	16.25%	17.32%	23.58%	29.25%	36.93%
	Minimum	0.77%	5.03%	4.78%	4.27%	5.16%	3.30%	17.34%
	End	3.30%	12.49%	12.98%	15.91%	21.20%	27.89%	35.12%

Table 12
Bolt force loss

PGA	EL-Centro		Wenchuan	
	Percentage	Force/kN	Percentage	Force/kN
0.07g	2.40%	2.35	0.89%	0.88
0.20g	1.46%	1.43	6.00%	5.88
0.40g	-	-	-1.99%	-1.95
0.51g	-	-	2.94%	2.88
0.62g	-	-	3.88%	3.80
0.80g	-	-	6.69%	6.55
1.0g	-	-	7.23%	7.07

Table 13
Cumulative losses of bolt force

PGA	EL-Centro		Wenchuan	
	Percentage	Force/kN	Percentage	Force/kN
0.07g	2.40%	2.35	3.30%	3.23
0.20g	6.49%	6.35	12.49%	12.23
0.40g	-	-	12.98%	12.70
0.51g	-	-	15.91%	15.58
0.62g	-	-	21.20%	20.75
0.80g	-	-	27.89%	27.30
1.0g	-	-	35.12%	34.38

4.6.2 Bolt forces of the intermediate column friction damper

The average initial bolt force, P_{ave}, is 98.785kN. The variations of average bolt force are listed on Table. 11. Positive values represent the decrease of bolt forces and negative values represent the increase of bolt forces. The losses of bolt forces at the beginning and end moments of each loading stage are listed in Table. 12. The accumulative losses of bolt force at the end of each loading stage are listed in Table. 13. The losses of bolt force are probably from the testing noises and installation errors as the CD only provides the lateral stiffness under 8-degree frequent earthquake (PGA = 0.07g). The friction damper in the CD slipped and the loss of bolt forces accumulates as the PGA is 0.2g. The maximum loss of bolt forces (PGA = 0.4g) is 16.25%, i.e. 12.70 kN at the end of testing. It can be found from Table.12 that the maximum loss was 6.0% in the conditions of as the PGA is 0.2g. The bolt force increase by 1.99% in the condition of 8-degree rare earthquake (PGA = 0.4g). The bolts provide stable and continuous pressure for the friction damper. Losses of bolt force are acceptable for the stability of CD under the 8-degree rare earthquake (PGA=0.51g). This implies that the friction damper is applicable in practical engineering. As shown in Table.13, the accumulative loss of bolt force is 12.98% decrease by 12.7kN after the action of 8-degree rare earthquake (PGA = 0.4g). It indicates that the friction damper of CD can withstand multiple aftershocks and the structural system functions properly.

5. Conclusions

A resilient prefabricated steel frame, PSC-CD, is innovatively developed from the PSC frame. The performance of the PSC-CD is compared to that of the PSC through carefully designed pseudo-dynamic testing. Conclusions are summarized as follows:

(1) The structural design and theoretical analysis of the PSC-CD are

conducted in the paper. The theoretical force-displacement curve of the PSC-CD is carefully proposed and validated through the testing. The testing specimens and experimental conditions are thoroughly discussed. The structural design method of the PSC-CD is feasible for the actual project.

(2) In the condition of 8-degree frequent earthquake (PGA = 0.07g), the interlayer drifts of both frames are less than the elastic interlayer limit (1/250). No gap-openings appear in the beam-column connections. The CD provides additional lateral stiffness to the steel frame. The friction damper of the CD in PSC-CD frame remain still. The force-displacement curves of the two systems are linear.

(3) In the condition of 8-degree fortification earthquake (PGA = 0.2g), the maximum inter-story drifts of PSC and PSC-CD are 1/129 and 1/150, beyond the elastic interlayer limit (1/250) but less than the plastic interlayer limit (1/50). Slight gap-opening occurs without residual rotation once unloading. The panel zones of PSC and PSC-CD reach the plastic state. The overall frames of both systems remain elastic states.

(4) In the condition of rare earthquake (PGA = 0.4g), the enclosed areas of the hysteresis curves further developed. The curve of PSC-CD is zigzag contributed by the friction damper of the CD. The energy-dissipation capacity and bearing capacity of PSC-CD is better than that of PSC. The beam-column connections are almost self-closed once unloading after the testing. The PSC-CD has much less residual gap-opening compared to that of the PSC. The losses of cable forces of the PSC-CD are smaller than that of the PSC as well.

(5) Before the fortification earthquake, the friction damper of the CD provides additional lateral stiffness to the frame without slippage. The CD provides damping function through the slippage of the friction damper as the seismic acceleration increases. The frictional blots of the friction damper increase the stability of the CD. Minor losses of bolt forces accumulate with the increase of seismic acceleration. The PSC-CD thus performs better than the PSC considering its stiffness and damping functions. This design of frame is applicable in the practical engineering.

References

The work presented in paper is supported by the Joint Program of Beijing Natural Science Foundation and Education Commission (Grant No. KZ201910016018) and Program for Changjiang Scholars and Innovative Research Team in University (IRT-17R06) .

References

[1] James M. Ricles,Richard Sause, Maria M. Garlock,Chen Zhao. Posttensioned seismic-resistant connections for steel frames. Journal of Structural Engineering, Vol. 127, No. 2, February, 2001.\

[2] J. M. Ricles, M. ASCE; R. Sause, S. W. Peng; and L. W. Lu. Experimental Evaluation of Earthquake Resistant Posttensioned Steel Connections. Journal of Structural Engineering, Vol. 128, No. 7, July 1, 2002.

[3] Ricles JM, Sause R, Peng SW, Lu LW. Experimental evaluation of earthquake resistant post-tensioned steel connections. J Struct Eng 2002;128(7): 850–9.

[4] Maria M. Garlock, James M. Ricles, Richard Sause. Experimental Studies of Full-Scale Posttensioned Steel Connections. Journal of Structural Engineering, Vol. 131, No. 3, March 1, 2005.

[5] Garlock M. Full-scale testing, seismic analysis, and design of post-tensioned seismic resistant connections for steel frames. Ph.D. dissertation, Civil and Environmental Engineering Dept., Lehigh Univ., Bethlehem, PA; 2002.

[6] Constantin Christopoulos; Andre Filiatrault, Chia-Ming Uang, and Bryan Folz. Posttensioned Energy Dissipating Connections for Moment-Resisting Steel Frames. Structural Engineering, Vol. 128, No. 9, September 1, 2002.

[7] P. Rojas; J. M. Ricles, R. Sause. Seismic Performance of Post-tensioned Steel Moment Resisting Frames With Friction Devices. Journal of Structural Engineering, Vol. 131, No. 4, April 1, 2005.

[8] Ying-Cheng Lin, James Ricles, Richard Sause, Choung-Yeol Seo. Earthquake simulations on a self-centering steel moment resisting frame with web friction devices. Structures 2009: Don't Mess with Structural Engineers © 2009 ASCE.

[9] Lin YC, Sause R, Ricles JM. Seismic performance of steel self-centering, moment-resisting frame: hybrid simulations under design basis earthquake. J Struct Eng 2013;139(11):1823–32.

[10] Federal Emergency Management Agency (FEMA)450. NEHRP recommended provisions for seismic regulations for new buildings and other structures. Part 1-provisions and Part 2-commentary. Washington, D.C.; 2003.

[11] Michael Wolski, A.M. ASCE, James M. Ricles, Richard Sause. Experimental Study of a Self-Centering Beam–Column Connection with Bottom Flange Friction Device. Journal of Structural Engineering, Vol. 135, No. 5, May 1, 2009.

[12] Feng X. Performance of research and engineering applications of the intermediate cylindrical friction damper. Southweat Jiaotong University.2012.

[13] Zhang Pengbo. Study on historical characteristics and evaluation method of shear damper (in Japanese).

[14] Suzui Kangzheng, satono Gangzhi, Nomura runnei hailianhe. Development and practicality of 4-sided friction. Dalin group technical research institute report no.752011 (in Japanese).

[15] Zhang AL, Zhang YX, Li R, Wang ZY. Cyclic behavior of a prefabricated self-centering beam–column connection with a bolted web friction device.Eng Struct 2016;111:185-198.

[16] Zhang YX, Wang ZY, Zhao W, Zhao WZ. A pseudo-dynamic test study on a self-centering prefabricated steel frame with a column base connected by semi-rigid joints. Adv Steel Const 2016;12(3):296-315.

[17] Zhang YX, Li QG, Zhuge Y, Liu AR, Zhao WZ. Experimental study on spatial prefabricated self-centering steel frame with beam-column connections containing bolted web friction devices. Eng Struct 2019;195:1-21.

[18] ZHANG Ailin, ZHANG Yanxia, ZHAO Wei, et al. Pseudo dynamic tests for a resilient prefabricated steel frame [J].Journal of Vibration and Shock, 2016, 35(05) : 207-215(in Chinese).

[19] ZHANG Yanxia, FEI Chenchao, NING Guang, et al. Dynamic elasto-plastic analysis on resilient prefabricated steel frame [J]. Journal of Vibration and Shock, 2016, 35(18) : 101 − 110 (in Chinese).

[20] ZHANG Ailin, ZHANG Yanxia, CHEN Yuanyuan, et al. Static pushover test on resilient prestressed steel frame with intermediate column containing friction dampers [J]. Journal of Building Structures, 2016, 37(3): 125-133 (in Chinese).

[21] GB 50011-2010 Code for seismic design of buildings. Beijing: China Architecture &Building Press, (in Chinese); 2016.

[22] Kumar S, Itoh Y, Saizuka K, Usami T. Pseudodynamic testing of scaled models. J Struct Eng 1997;123(4):524-6.

[23] JGJ82-2011, Technical specifications for high strength bolt connections of steel structures. Beijing: China Architecture & Building Press (in Chinese).

[24] GB50017-2017, Standard for design of steel structures. Beijing: China Architecture & Building Press. [in Chinese].

[25] GB50019-2017, Standards for design of steel buildings. Beijing: China Architecture & Building Press; 2016 (in Chinese).